ROBUST GROUNDNUT LEAF DISEASE DETECTION USING ORCA PREDATION ALGORITHM WITH TWO-TIER DEEP TRANSFER LEARNING MODEL

G. Suresh[1], K. Seetharaman[2]

Article History: Received: 16.01.2023 **Revised:** 01.03.2023 **Accepted:** 14.04.2023

Abstract

Groundnut is one of the important oilseed crops worldwide, and India is ranked as the second-biggest producer of groundnuts. This crop can be affected by numerous diseases, which are key considerations contributing to quality degradation and productivity loss. Therefore, designing more reliable and automated solutions using machine learning (ML) and deep learning (DL) models to detect groundnut leaf disease becomes essential. With this motivation, this study presents a Robust Groundnut Leaf Disease Detection using Orca Predation Algorithm with Deep Learning (RGLDD-OPADL) method. The RGLDD-OPADL algorithm focuses on the classification and recognition of groundnut leaf diseases. In the presented RGLDD-OPADL method, different stages of operations are involved. To do this, the presented RGLDD-OPADL technique comprises median filtering (MF) approach to eliminate the noise. Besides, the SqueezeNet model is used to extract a set of features. The RGLDD-OPADL technique exploits the deep recurrent neural network (DRNN) model for disease detection and classification. Finally, the OPA-based hyperparameter optimization approach is utilized to select the DRNN parameters. The experimental outcomes of the RGLDD-OPADL methodology are tested on a benchmark dataset. The comprehensive comparison analysis portrayed the enhanced performance of the RGLDD-OPADL method in terms of different measures.

Keywords: Groundnut leaf disease; Orca predation algorithm; Deep learning; Computer vision; Parameter tuning

[1,2]Department of Computer and Information Science, Annamalai University, Chidambaram, Tamil Nadu, India

Email: [1]suresh2023phd@gmail.com, [2]kseethaddeau@gmail.com

DOI: 10.31838/ecb/2023.12.1.569

1. Introduction

Agriculture is undoubtedly the primary source of food, employment, and income and an essential economic supplier. Infections and plant diseases from pests might affect the worldwide economy by decreasing the quality and production of food [1]. For preventing endemics and epidemics, Prophylactic treatments are ineffective. Proper detection and timely monitoring of plant disease utilizing an appropriate crop protection mechanism might prevent loss in the quality of production [2]. Categorizing kinds of plant diseases is very significant and has been a big concern. Prior identification of plant diseases resulted in superior decisions in handling agricultural productivity. Diseased plants usually have prominent spots or marks on the leaves, flowers, stems, or fruits [3]. Notably, all infections leave unique patterns, which help to find abnormalities. Recognizing plant disease necessitates a workforce and expertise. Still, manually analyzing the plant infection is time-consuming and subjective, and, rarely, the disease recognized by experts or farmers may be inaccurate [4,5]. It could result in using an inappropriate pesticide in evaluating plant diseases that worsen crop quality and pollute nature. Groundnut is a crop with many benefits and rich nutrition. In China, being the main economic and oil crop had a large growing area and ranks as the second-largest crop cultivated in China [6].

The complicated field environment of this crop caused the leaves to be affected easily by pathogens. The pathogens can rapidly spread via natural elements and have higher reproduction capabilities. The critical element, which affects reproduction, is the humidity of groundnuts in the phase called seedling. The disease of groundnut leaves could lessen the quality and production of this crop by damaging the chlorophyll and green tissue presented in the leaves [7]. Artificial detection of groundnut-leaf disease necessitates the knowledge of experts, and it becomes easier to misdiagnose them by artificial visual analysis. Thus, groundnut disease could not be treated and identified in time. The solution to controlling groundnut diseases is to detect the disease category precisely and rapidly and initiate preventive measures in time [8].

The growth in plant disease identification was massive and denotes an enormous development in research with the deep learning (DL) and machine learning (ML) approaches. It made it simple for automatic feature extraction and classification for expressing the original image features [9]. Moreover, the accessibility of GPU machines, data, and software supporting complicated DL structures with less difficulty has made it possible to switch from conventional approaches to the DL method [10]. Today, convolution neural networks (CNN) have grabbed more interest for their classification and detection capabilities that work by mining lower-level complicated features from images. Later, CNN was chosen to replace conventional approaches in automatic plant disease detection as they attained superior results [11].

This study presents a Robust Groundnut Leaf Disease Detection utilizing Orca Predation Algorithm with Deep Learning (RGLDD-OPADL) methodology. The focus of the RGLDD-OPADL approach lies in the recognition and classification of groundnut leaf diseases. The presented RGLDD-OPADL technique comprises median filtering (MF) approach to eliminate the noise. Besides, the SqueezeNet model is employed to extract a set of features. The RGLDD-OPADL method applies the deep recurrent neural network (DRNN) model for disease detection and classification. Finally, the OPA-based hyper-parameter optimization approach is utilized to select the DRNN parameters. The outcomes of the RGLDD-OPADL technique are tested on a benchmark dataset.

Related Works

Suresh and Seetharaman [12] have proposed an Automated Groundnut Leaf Disease Recognition approach utilizing WOA with DL (AGLDR-WOADL). It has a sequence of operations to detect the diseased portions of the image, such as threshold-based segmentation, feature extraction, and classification. For feature extraction, the NASNet approach has been employed. Eventually, the WOA with LSTM methods has been applied to classify diverse types of plant diseases. Devi et al. (2020) [13] have proposed a method H2K which fuses the Harris corner detector, HOG (Histogram on Oriented Gradient) and KNN classifier for accurate and automatic detection and classification of groundnut leaf diseases. Feng et al. [14] presented an online detection approach for peanut leaf diseases that depends on the DTL and data balance method. The data balance technique was used to overcome the data distribution tilt problem. Likewise, TL has been utilized for framing a peanut leaf disease detection approach for enriching the generalization capability depending on the lightweight CNN. Vaishnnave et al. [15] modelled a potential scheme of DCNN as it automatically identifies the significant features without human supervision. The DCNN process can intensely identify plant disease with a DL method. Likewise, the DCNN testing and training procedure exhibits a precise groundnut disease classification and determination outcome. Dong et al. [16] implemented and designed a unique

approach to finding peanut leaf disease images by considering capsule networks. Initially, building the peanut leaf disease imageries dataset and data enhancement has been utilized for processing the images. Also, this study devised two kinds of capsule networks: altering the variables for peanut leaf disease imageries and stacking three convolution layers to the original method. Vaishnnave et al. [17] have presented a method that performs image acquisition, image pre-processing, segmentation, features extraction and classification using KNN; they reported that it enhances crop productivity.

The Proposed Model

In this research work, we have concentrated on the design and development of the RGLDD-OPADL technique for identifying and classifying groundnut leaf diseases. In the presented RGLDD-OPADL technique, different stages of operations are involved, such as MF-based noise elimination, SqueezeNet feature extraction, DRNN classification, and OPA-based hyperparameter tuning. Fig. 1 demonstrates the overall flow of the RGLDD-OPADL algorithm.

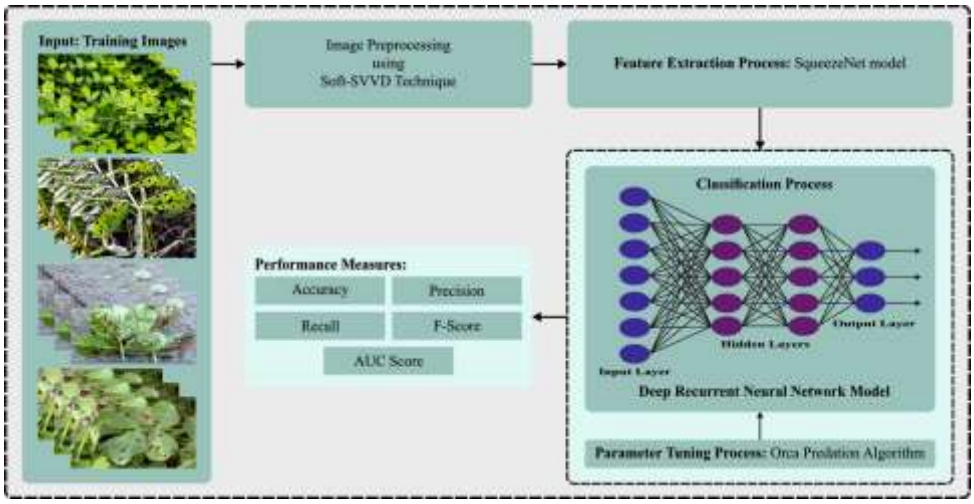

Fig. 1. Overall flow of RGLDD-OPADL approach.

Pre-processing

Generally, while photographing the plants there are many possibilities of adding noise in the images. Therefore, the proposed system applies a pre-processing technique, soft-SVVD [18], to reduce the effects of the noise in the image. The main objective of the soft-SVVD is to recognise the noised pixels in the feature space. The recognised noised pixels are replaced by median values of the normal pixels. The denoising method is depicted in Eq. (1), which enhances the proposed RGLDD-OPADL method even if the image is severely affected by various kinds of noises. In order to identify the abnormal pixels in the image, the given input image is divided into sliding windows of size, 3×3.

$$\left\| p_{k,l} - C_{k,l} \right\|^2 \le r^2 \quad (1)$$

where, $\|.\|$ is the Euclidean norm; $C_{k,l}$ is the mean entropy value of the pixels in the window, which is calculated based on the expression in Eq. (2).

$$C_{k,l} = \sum_{u=1}^{m+n} \lambda_u \theta\left(p_{k,l} \right) \quad (2)$$

λ_u denotes the Lagrange multiplier; $\theta\left(p_{k,l}\right)$ is a vector form of the pixel entropy values; $p_{k,l}$ is the entropy value of the pixel to be classified that whether it is noised or not.

To classify the pixel, $p_{k,l}$, the distance between the $p_{k,l}$ and $C_{k,l}$ is calculated. If it is less than or equals to radius, *r*, then $p_{k,l}$ is accepted as a normal pixel; otherwise, it is recognised as abnormal. In terms of statistical terminology, the $C_{k,l}$ represents the mean of the pixels in the window; *r* represents the standard deviation of the pixels in the window.

Feature Extraction Using Squeezenet Model

This paper uses the SqueezeNet method to produce a collection of feature vectors. The principle of SqueezeNet is to maintain low accuracy with fewer parameters. Three practical approaches were adopted to accomplish the flaws above-mentioned [19]. Initially, the 3x3 convolutional size was replaced by the 1x1 convolutional size, which has lesser parameters. Next, the input channels to the 3x3 convolutional size are decreased. Lastly, a subsampled operation was implemented to make

the convolutional layer with larger activation. SqueezeNet drew on the concept of the Inception model to develop a Fire module with an expanded layer and the squeeze layer. Fig. 2 displays the structure of the SqueezeNet model. The squeeze layer applied 1x1 filters to compress the input components to decrease the channels for input components. The expansion layer applied the 1x1 and 3x3 filters for multi-scale learning and concatenating. The size of the input feature map is h × w × n.

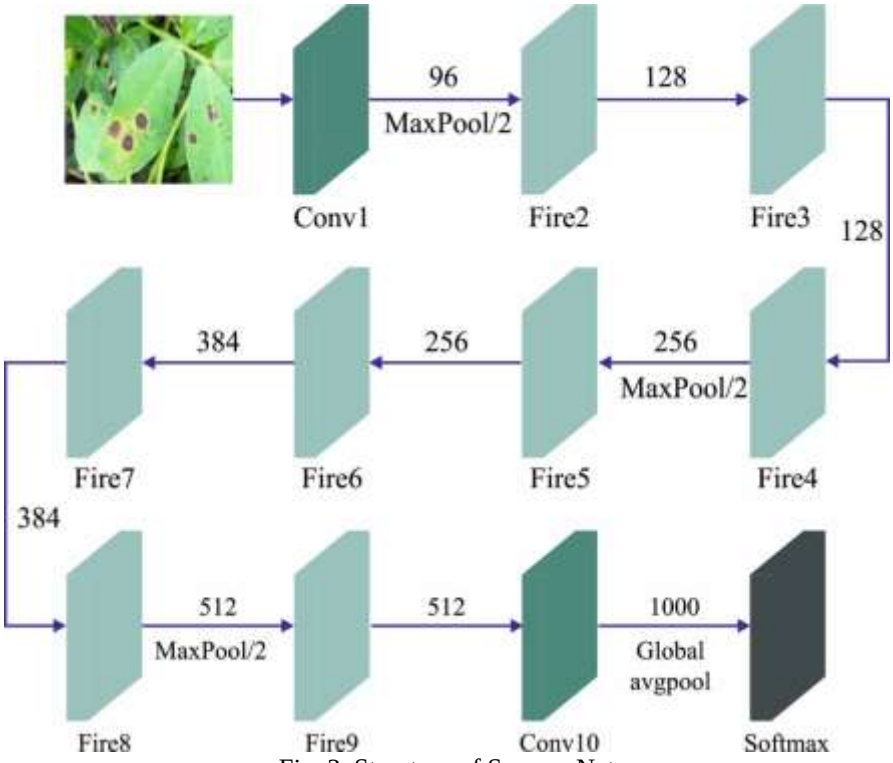

Fig. 2. Structure of SqueezeNet

Initially, the input feature map passes over the squeeze layer and attains the output feature map with the h × w × s1 size. Though the size of the feature map remains the same, the channel is reduced from n to s1. The output feature map of the squeeze layer is transferred into 1x1 and 3x3 filters in expand layer, correspondingly. Next, concatenate the outcome of convolution. Lastly, the channels change to e1 + e3. In order to allow the output activation of 1x1 and 3x3 convolution sizes of the extension model to have similar width and height, the boundary zero filling function with 1 pixel was implemented for the input of 3x3 convolution sizes in the extension model. Rectified Linear Unit (ReLU) is employed to expand the layer and activation of squeeze layer. In the meantime, there is no fully connected layer in SqueezeNet.

Groundnut Leaf Disease Detection Using DRNN Model

To detect and classify groundnut leaf disease, the DRNN model is used [20]. The G extracted feature from Twitter is inputted into the model. In the presented method, the recurrent connection is just in the hidden state. The major benefit of using the algorithm is that it effectively implements the classifier technique even at a dissimilar feature length about the data series. The initial dataset is inputted into the current prediction and continues the iteration with data related to the hidden layer. The architecture of DRNN classification was made based on the output vector of p^{th} layer at s^{th} time as $S^{(p,s)} = \{S_1^{(p,s)}, S_2^{(p,s)}, \ldots S_l^{(p,s)}, \ldots S_q^{(p,s)}\}$and the input vector of p^{th} layer at s^{th} time as $G^{(p,s)} = \{G_1^{(p,s)}, G_2^{(p,s)}, \ldots G_l^{(p,s)}, \ldots G_q^{(p,s)}\}$, correspondingly. As a result, the pair of each element of the output and input vectors are termed units. Here, l represents the arbitrary value of p^{th} layer and q illustrates the total amount of components of the p^{th} layer. Together with the aforementioned variable, the arbitrary amount of $(p-1)^{th}$ layers are represented by a and the overall amount of units of $(p-1)^{th}$ layer is represented by e, correspondingly. In addition, the recurrent weight of p^{th} layer is represented as $w^{(p)} \in B^{q \times I}$, and the input propagation weight from $(p-1)^{th}$ layer to p^{th} layer is indicated as $W^{(p)} \in B^{q \times I}$ and B shows the set of weights. Moreover, the mathematical

expression of input vector is represented as follows:

$$G_l^{(p,S)} = \sum_{b=1}^{I} x_{lb}^{(p)} S_b^{(p-1S)} + \sum_{l}^{q} h_{ll}^{(p)} S_{l'}^{(p,s-1)} \quad (3)$$

Where $x_{lb}^{(p)}$ and $h_{ll'}^{(p)}$ represents the element of $W^{(p)}$ and $w^{(p)}$. l' denotes the arbitrary number of p^{th} layer and the element of output vector of the p^{th} layer is expressed as follows:

$$S_l^{(p,s)} = \alpha^{(p)}\left(G_l^{(p,s)}\right) \quad (4)$$

Where α denotes the activation function. Moreover, the logistic sigmoid function as $(G) = \frac{1}{(1+e^{-G})}$, the ReLU as $\alpha(G) = \max(G, \eta)$ and the activation function such as sigmoid function as $(G) = \tanh(G)$ are commonly used activation functions.

In order to make the classification simple, assume η^{th} unit as $S_\eta^{(p-1,s)}$ and η^{th} weight as $x_{l\eta}^{(p)}$, and the bias is indicated as follows:

$$S^{(p,s)} = \alpha^{(p)}.\left(W^{(p)} S^{(p-1,s)} + w^{(p)}.S^{(p,S-1)}\right) \quad (5)$$

Here, $S^{(p,s)}$ denotes the classification output. For hyperparameter tuning process, the OPA is used. Orcas are extremely clever and are extremely socialized carnivore that belongs to the dolphin family [21]. In OPA, a set of N orcas was generated. The orcas swim in 1D, 2D, 3D, and multi-dimensional spaces. The mathematical expression can be represented as:

$$K = [k1, k2, \ldots, kN] = \begin{bmatrix} & k1,1 & k1,2 & \ldots & k1,D & \\ \vdots & k2,1 & k2,2 & \ldots & k2,D & \vdots \\ & kN,1 & kN,2 & \ldots & k3,D & \end{bmatrix} \quad (6)$$

In Eq. (6), D indicates the dimension of decision variable, K refers to the population of orca that shows the set of potential outcomes for the given issue, and kN depicts position of N^{th} orca that represents solution of the N^{th} candidate positioned at the given problem. Once orcas stumble on a shoal of fish, they collaborate and send data to each other through sonar technology. Thereby, forcing the target to move towards the safer region for hunting. Moreover, these activities are divided into two stages such as surrounding and driving prey. Hence, $p1$ parameter is added to modify the orca's probability of carrying out those operations separately. The $p1$ value can be selected within the range [0,1]. Once the random value is higher than $p1$, the driving stage can be performed; or else, the encircling stage can be performed. While they spot one, Orcas need to pursue a shoal of fish. Furthermore, the individual orcas approach the prey, thereby regulating the orca group's central location to retain their nearby location to prey and prevent the diversion from the objective of orca groups. The initial strategy can be utilized once the orca group is bigger (rand $> q$). the next strategy is used once the orca group is smaller ($rand \leq q$). The position and movement speed can be described as follows:

$$v_{chase,1,i}^t = z \times \left(g \times x_{best}^t - F \times (y \times M^t + w \times x_i^t)\right) \quad (7)$$

$$v_{chase,2,i}^t = e \times x_{best}^t - x_i^t \quad (8)$$

$$M = \frac{\Sigma_{i=1}^{N} x_i^t}{N} \quad (9)$$

$$c = 1 - b \quad (10)$$

$$\begin{cases} v_{chase,1,i}^t = x_i^t + v_{chase,1,i}^t & rand > q \\ v_{chase,2,i}^t = x_i^t + v_{chase,2,i}^t & rand \leq q \end{cases} \quad (11)$$

Wherex_i^t denotes the existing particles location, g denotes global optimum location, $v_{chase,1,i}^t$ and $v_{chase,2,i}^t$ characterizes the chasing speed of i^{th} orca at t time afterward choosing the initial and the second chasing strategies, correspondingly, t represents the amount of cycles, e refers to a random integer whose value ranges between [0,2], $rand$ denotes the uniformly distributed random value number within [0,1]. M shows the average position of orca; F denotes the constant whose value is 2. Many studies decided that the better value of q with respect to performance is ~ 0.9 meanwhile q ranges from zero to one, x_{besi}^t denotes the location of fittest particle. Orcas form controlled spheres around the school of fish once the shoal is brought to the surface. Orcas interact

with each other using sonar all over the encirclement and calculate the future movement position based on the location of surrounding orcas.

Assume those orcas self-locate related to the location of arbitrarily chosen orcas, and calculate the position as:

$$x_{chase,3,i}^{t} = x_{j1,k}^{t} + u \times \left(x_{j2,k}^{t} - x_{j3,k}^{t}\right) \quad (12)$$

change their present position. When the orcas spot the fish getting closer while they were still monitoring the novel location, they still continue; if not, they stay in the prior spot which can be described by:

$$\begin{cases} x_{chase,i}^{t} = x_{chase,i}^{t} & f(x_{chase,i}^{t}) < f(x_{i}^{t}) \\ x_{chase,i}^{t} = x_{i}^{t} & f(x_{chase,i}^{t}) \geq f(x_{i}^{t}) \end{cases} \quad (13)$$

In Eq. (12), Max_{ter} represents the maximal amount of iterations, $j1, j2, j3$ denotes the three randomly selected orcas from N orcas and $j1 \neq j2 \neq j3$, $x_{chase,3,i}^{t}$ indicates the position of the i^{ih} orca. Sonar allows orcas to discover their prey and

In Eq. (13), $f(x_i^t)$ denotes the fitness function with respect to x_i^t, $f(x_{chase,i}^t)$ indicates the fitness function value related to $x_{chase,i}^t$. An assumption of four orcas has been made, as more orcas will lead the method to take longer to reach its convergence that relates to the four better positions to strike in the circle.

Once the orcas try to enter the area, they should follow the path of the 4 orcas that are existing already. The position and movement speed during the assault was calculated as follows:

$$v_{attack,1,i}^{t} = \frac{x_{first}^{t} + x_{first}^{t} + x_{third}^{t} + x_{four}^{t}}{4 - x_{chase,i}^{t}} \quad (14)$$

$$v_{attack,2,i}^{t} = \frac{x_{chase,j1}^{t} + x_{chase,J2}^{t} + x_{chase,j3}^{t}}{3 - x_{i}^{t}} \quad (15)$$

$$x_{attack,i}^{t} = x_{chase,i}^{t} + g1 \times v_{attack,1,i}^{t} + g2 \times v_{attack,2,i}^{t} \quad (16)$$

Where $v_{attack,2,i}^{t}$ denotes the i^{ih} velocity vector while returning to containment at t time and $v_{aiiack,1,i}^{t}$ signifies the i^{th} velocity vector while hunting prey at t time. The four orcas' better location can be denoted by $x_{first}^{t} x_{second}^{t}$, x_{ihird}^{t}, x_{four}^{t} correspondingly $j1 \neq j2 \neq j3$, $x_{attack,i}^{t}$ shows the position of i^{ih} orca at t time, $g1$ and $g2$ denotes the random integer within[0,2]. Orca uses sonar to seek food and modify their position in the same way as how they chase. The orca's location can be assigned the problem's possible range's minimal limit value (lb). The OPA method makes fitness function (FF) extraction to acquire improved classifier outcomes, and it sets positive values that represent better outcomes for the candidate solution. In the presented method, the decline in the classifier error rate is considered a FF.

$$fitness(x_i) = ClassifierErrorRate(x_i) = \frac{number\ of\ misclassified\ samples}{total\ number\ of\ samples} * 100 \quad (17)$$

2. Results and Discussion

This section discusses the groundnut disease detection results of the RGLDD-OPADL algorithm on a dataset comprising 774 samples, as provided in Table 1. Fig. 3 represents the sample images. The confusion matrices of the RGLDD-OPADL method on groundnut disease detection results are given in Fig. 4. The outcomes indicate that the RGLDD-OPADL technique obtains effectual performance with maximum groundnut disease detection results.

Table 1 Details of database

Class	No. of Sample Images
Early Leaf	228
Rust	96
Necrosis	120

Blight	114
Healthy Leaf	60
Late Spot	156
Total Number of Sample Images	**774**

Fig. 3. Sample images

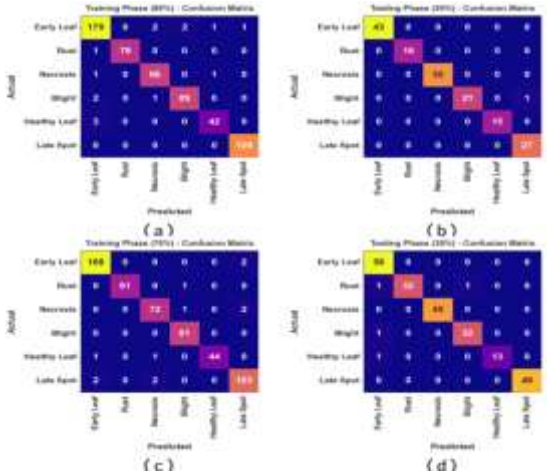

Fig. 4. Confusion matrices of RGLDD-OPADL approach (a-b) 80:20 of TRP/TSP and (c-d) 70:30 of TRP/TSP

In Table 2 and Fig. 5, the groundnut disease detection outcomes of the RGLDD-OPADL system are examined on 80:20 of TRP/TSP. The results highlighted that the RGLDD-OPADL technique recognizes six types of diseases. For instance, with 80% of TRP, the RGLDD-OPADL approach provides average $accu_y$, $prec_n$, $reca_l$, F_{score}, and AUC_{score} of 99.19%, 97.56%, 97.22%, 97.38%, and 98.35% respectively. Eventually, with 20% of TSP, the RGLDD-OPADL method provides average $accu_y$, $prec_n$, $reca_l$, F_{score}, and AUC_{score} of 99.78%, 99.40%, 99.24%, 99.31%, and 99.56% correspondingly.

Table 2 Groundnut disease detection outcome of RGLDD-OPADL technique on 80:20 of TRP/TSP

Class	$Accu_y$	$Prec_n$	$Reca_l$	F_{score}	AUC_{score}
Training Phase (80%)					
Early Leaf	97.90	96.24	96.76	96.50	97.57
Rust	99.84	100.00	98.75	99.37	99.38
Necrosis	99.19	96.63	97.73	97.18	98.58
Blight	99.19	97.80	96.74	97.27	98.18
Healthy Leaf	99.19	95.45	93.33	94.38	96.49
Late Spot	99.84	99.23	100.00	99.61	99.90

Average	**99.19**	**97.56**	**97.22**	**97.38**	**98.35**
Testing Phase (20%)					
Early Leaf	100.00	100.00	100.00	100.00	100.00
Rust	100.00	100.00	100.00	100.00	100.00
Necrosis	100.00	100.00	100.00	100.00	100.00
Blight	99.35	100.00	95.45	97.67	97.73
Healthy Leaf	100.00	100.00	100.00	100.00	100.00
Late Spot	99.35	96.43	100.00	98.18	99.61
Average	**99.78**	**99.40**	**99.24**	**99.31**	**99.56**

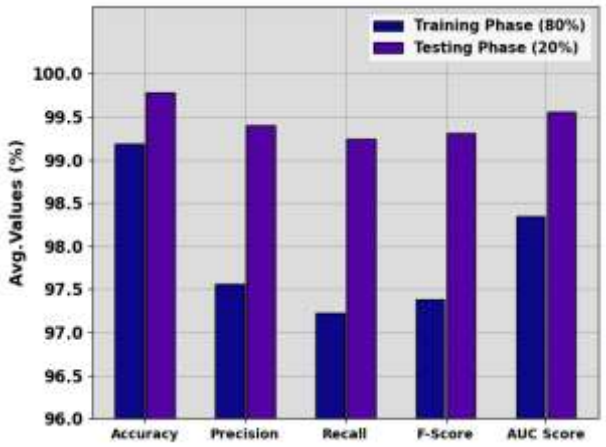

Fig. 5. Average outcome of RGLDD-OPADL technique on 80:20 of TRP/TSP

In Table 3 and Fig. 6, the groundnut disease detection outcomes of the RGLDD-OPADL method are examined on 70:30 of TRP/TSP. The results emphasized that the RGLDD-OPADL method recognizes six types of diseases. For example, with 70% of TRP, the RGLDD-OPADL method offers average $accu_y$, $prec_n$, $reca_l$, F_{score}, and AUC_{score} of 99.26%, 98.02%, 97.52%, 97.76%, and 98.53% correspondingly. Finally, with 30% of TSP, the RGLDD-OPADL method provides average $accu_y$, $prec_n$, $reca_l$, F_{score}, and AUC_{score} of 99.43%, 98.68%, 97.32%, 97.95%, and 98.48% correspondingly.

Table 3 Groundnut disease detection outcome of RGLDD-OPADL technique on 70:30 of TRP/TSP

Class	**$Accu_y$**	**$Prec_n$**	**$Reca_l$**	**F_{score}**	**AUC_{score}**
Training Phase (70%)					
Early Leaf	99.08	98.25	98.82	98.53	99.01
Rust	99.82	100.00	98.39	99.19	99.19
Necrosis	98.89	96.00	96.00	96.00	97.68
Blight	99.63	97.59	100.00	98.78	99.78
Healthy Leaf	99.63	100.00	95.65	97.78	97.83
Late Spot	98.52	96.26	96.26	96.26	97.67
Average	**99.26**	**98.02**	**97.52**	**97.76**	**98.53**
Testing Phase (30%)					
Early Leaf	98.71	95.08	100.00	97.48	99.14
Rust	99.14	100.00	94.12	96.97	97.06
Necrosis	100.00	100.00	100.00	100.00	100.00
Blight	99.14	96.97	96.97	96.97	98.23
Healthy Leaf	99.57	100.00	92.86	96.30	96.43
Late Spot	100.00	100.00	100.00	100.00	100.00
Average	**99.43**	**98.68**	**97.32**	**97.95**	**98.48**

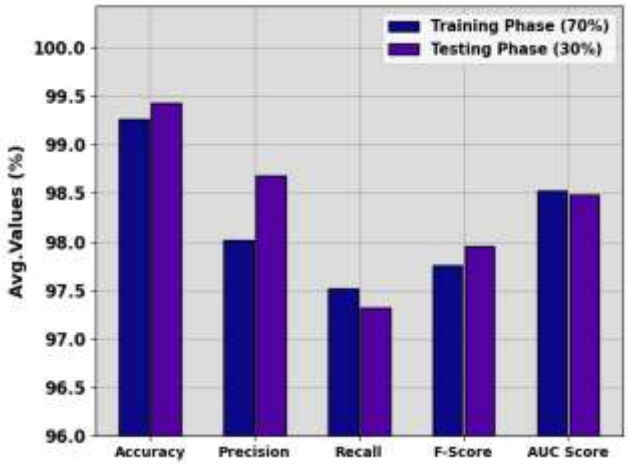

Fig. 6. Average outcome of RGLDD-OPADL technique on 70:30 of TRP/TSP

Fig. 7 exhibits the classifier results of the RGLDD-OPADL method at 80:20 and 70:30. Figs. 7a-7c reveals the accuracy analysis of the RGLDD-OPADL technique under 80:20 and 70:30. The figure noted that the RGLDD-OPADL method reached higher accuracy values over increasing epochs. The increasing validation accuracy over training accuracy also displays that the RGLDD-OPADL method learns efficiently on the test dataset. Lastly, Figs. 7b-7d demonstrates the loss study of the RGLDD-OPADL technique under 80:20 and 70:30. The outcomes specify that the RGLDD-OPADL method reaches closer training and validation loss values. The RGLDD-OPADL technique learns efficiently on the test dataset.

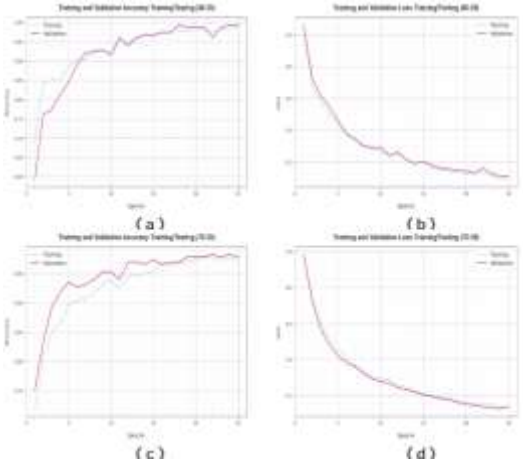

Fig. 7. (a-c) Accuracy curve on 80:20 and 70:30 and (b-d) Loss curve on 80:20 and 70:30

Fig. 8 validates the classifier results of the RGLDD-OPADL method at the ratio of 80:20 and 70:30. Figs. 8a-8c exhibits the PR curve analysis of the RGLDD-OPADL approach under 80:20 and 70:30. The outcomes specified that the RGLDD-OPADL method increased PR values. Furthermore, the RGLDD-OPADL system can attain higher PR values in all classes. Lastly, Figs. 8b-8d demonstrates the ROC analysis of the RGLDD-OPADL method under 80:20 and 70:30. The figure defined that the RGLDD-OPADL method resulted in improved ROC values. Further, the RGLDD-OPADL system can extend enhanced ROC values on all classes.

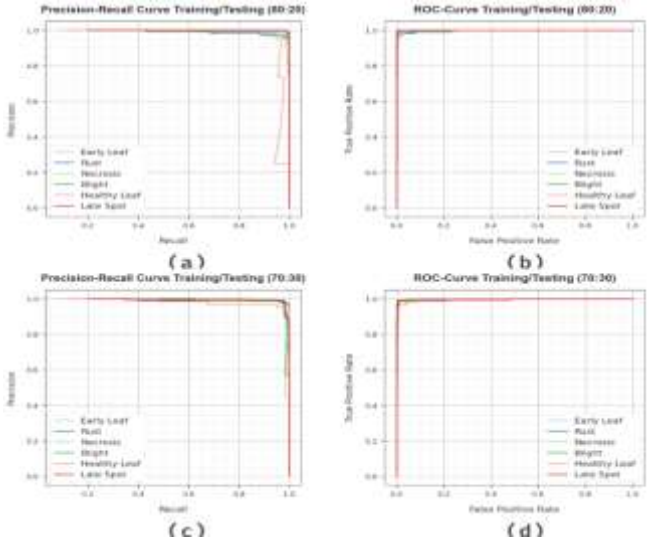

Fig. 8. (a-c) PR curve on 80:20 and 70:30 and (b-d) ROC curve on 80:20 and 70:30

Finally, an extensive comparative examination of the RGLDD-OPADL technique with recent approaches is made in Fig. 9 [15]. Based on $accu_y$, the RGLDD-OPADL technique gains improving $accu_y$ of 99.78% while the PCA_FSCABC, FRFE_IHGA, WE_BBO, PCA_kSVM, and DCNN models accomplish decreasing $accu_y$ of 88.76%, 88.84%, 89.64%, 89.49%, 88.24%, and 95.31% respectively. Meanwhile, based on $prec_n$, the RGLDD-OPADL method gains improving $prec_n$ of 99.40% while the PCA_FSCABC, FRFE_IHGA, WE_BBO, PCA_kSVM, and DCNN methods accomplish decreasing $prec_n$ of 86.70%, 86.95%, 89.91%, 86.86%, 86.99%, and 92.59% correspondingly. Concurrently, based on $reca_l$, the RGLDD-OPADL method gains improving $reca_l$ of 99.24% while the PCA_FSCABC, FRFE_IHGA, WE_BBO, PCA_kSVM, and DCNN methods accomplish decreasing $reca_l$ of 89.02%, 88.40%, 89.21%, 87.12%, 89.11%, and 95.27% correspondingly. Finally, based on F_{score}, the RGLDD-OPADL method advances improving F_{score} of 99.31% while the PCA_FSCABC, FRFE_IHGA, WE_BBO, PCA_kSVM, and DCNN approaches accomplish decreasing F_{score} of 88.22%, 88.75%, 88.70%, 89.78%, 90.06%, and 93.29% correspondingly.

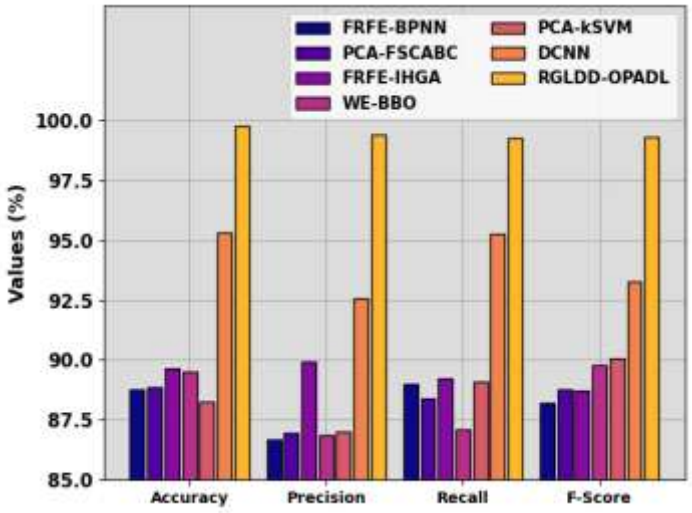

Fig. 9. Comparative outcome of RGLDD-OPADL approach with other systems

3. Conclusion

In this study, we have concentrated on the design and development of the RGLDD-OPADL technique for the identification and classification of groundnut leaf diseases. In the presented RGLDD-OPADL technique, different stages of operations are involved such as MF based noise elimination, SqueezeNet feature extraction, DRNN classification, and OPA based hyperparameter

tuning. In this work, SqueezeNet model is used to extract a useful set of feature extractors. For disease detection and classification, the RGLDD-OPADL technique exploits the DRNN model. Finally, the OPA based hyperparameter optimization approach is utilized for optimal selection of the DRNN parameters. The experimental outcomes of the RGLDD-OPADL system are tested on benchmark dataset. The comprehensive study stated the enhanced performance of the RGLDD-OPADL approach in terms of different measures.

4. References

1. Suresh, G. and Seetharaman, K., 2023. Real-time automatic detection and classification of groundnut leaf disease using hybrid machine learning techniques. Multimedia Tools and Applications, 82(2), pp.1935-1963.
2. Patayon, U.B. and Crisostomo, R.V., 2022. Peanut leaf spot disease identification using pre-trained deep convolutional neural network. International Journal of Electrical and Computer Engineering, 12(3), p.3005.
3. Selvakumar, V. and Seetharaman, K., 2023. HOML-SL: IoT Based Early Disease Detection and Prediction for Sugarcane Leaf using Hybrid Optimal Machine Learning Technique, Journal of Survey in Fisheries Sciences 10(2S), 3284-3309
4. Malaisamy, J. and Rethnaraj, J., 2023. Smart Nutrient Deficiency Prediction System for Groundnut Leaf. Intelligent Automation & Soft Computing, 36(2).
5. Seetharaman, K., Mahendran, T., 2023. Leaf Disease Detection in Banana Plant using Gabor Extraction and Region-Based Convolution Neural Network (RCNN). J. Inst. Eng. India Ser. A **103**, pp. 501–507.
6. Anbumozhi, A. and Shanthini, A., 2023. Leaf Diseases Identification and Classification of Self-Collected Dataset on Groundnut Crop using Progressive Convolutional Neural Network (PGCNN). International Journal of Advanced Computer Science and Applications, 14(2).
7. Rajmohan, M., Reddy, D.S.S., Krishna, C.M. and Krishna, N.M.S., 2022, October. Groundnut leaf disease identification using image processing. In AIP Conference Proceedings (Vol. 2519, No. 1, p. 030110). AIP Publishing LLC.
8. Janani, M. and Jebakumar, R., 2023. Detection and classification of groundnut leaf nutrient level extraction in RGB images. Advances in Engineering Software, 175, p.103320.
9. Xu, L., Cao, B., Ning, S., Zhang, W. and Zhao, F., 2023. Peanut leaf disease identification with deep learning algorithms. Molecular Breeding, 43(4), p.25.
10. Rakholia, R.M., Tailor, J.H., Saini, J.R., Kaur, J. and Pahuja, H., 2022. Groundnuts Leaf Disease Recognition using Neural Network with Progressive Resizing. International Journal of Advanced Computer Science and Applications, 13(6).
11. Qi, H., Liang, Y., Ding, Q. and Zou, J., 2021. Automatic identification of peanut-leaf diseases based on stack ensemble. Applied Sciences, 11(4), p.1950.
12. Suresh, G. and Seetharaman, K., 2022, November. Automated Groundnut Leaf Disease Recognition Using Whale Optimization Algorithm with Deep Learning Model. In 2022 International Conference on Augmented Intelligence and Sustainable Systems (ICAISS) IEEE Xplore, pp. 310-315.
13. Devi, K.S., Srinivasan, P. and Bandhopadhyay, S., 2020. H2K–A robust and optimum approach for detection and classification of groundnut leaf diseases. Computers and Electronics in Agriculture, 178, p.105749.
14. Feng, Q., Xu, P., Ma, D., Lan, G., Wang, F., Wang, D. and Yun, Y., 2022. Online recognition of peanut leaf diseases based on the data balance algorithm and deep transfer learning. Precision Agriculture, pp.1-27.
15. Vaishnnave, M.P., Suganya Devi, K. and Ganeshkumar, P., 2020. Automatic method for classification of groundnut diseases using deep convolutional neural network. Soft Computing, 24, pp.16347-16360.
16. Dong, M., Mu, S., Su, T. and Sun, W., 2019. Image recognition of peanut leaf diseases based on capsule networks. In Artificial Intelligence: Second CCF International Conference, ICAI 2019, Xuzhou, China, August 22-23, 2019, Proceedings 2 (pp. 43-52). Springer Singapore.
17. Vaishnnave, M.P., Devi, K.S., Srinivasan, P. and Jothi, G.A.P., 2019, March. Detection and classification of groundnut leaf diseases using KNN classifier. In 2019 IEEE International Conference on System, Computation, Automation and Networking (ICSCAN) (pp. 1-5). IEEE.
18. Vasanthi, M. and Seetharaman, K., 2022. Facial Image Recognition for Biometric Authentication Systems Using A

Combination of Geometrical Feature Points and Low-level Visual Features, Journal of King Saud University – Computer and Information Sciences, 34(7), pp. 4109-4121.

19. Liu, Y., Li, Z., Chen, X., Gong, G. and Lu, H., 2020, May. Improving the accuracy of SqueezeNet with negligible extra computational cost. In 2020 International Conference on High Performance Big Data and Intelligent Systems (HPBD&IS) (pp. 1-6). IEEE.

20. Fan, C., Wang, J., Gang, W. and Li, S., 2019. Assessment of deep recurrent neural network-based strategies for short-term building energy predictions. Applied energy, 236, pp.700-710.

21. Khan, N.M., Ahmed, A., Haider, S.K., Zafar, M.H., Mansoor, M. and Akhtar, N., 2023. Hybrid General Regression NN Model for Efficient Operation of Centralized TEG System under Non-Uniform Thermal Gradients. Electronics, 12(7), p.1688.